Romanian Reports in Physics **XX**, XYZ (2020)

COMMISSIONING EXPERIMENT ON LASER-PLASMA ELECTRON ACCELERATION IN SUPERSONIC GAS JET AT CETAL-PW LASER FACILITY

C. DIPLASU, G. GIUBEGA, R. UNGUREANU, G. COJOCARU, M. SERBANESCU, A. MARCU, E. STANCU, A. ACHIM AND M. ZAMFIRESCU

CETAL, National Institute for Laser, Plasma and Radiation Physics, P.O. Box MG-36, RO 077125, Magurele- Bucharest, Romania
E-mails: constantin.diplasu@inflpr.ro; georgiana.giubega@inflpr.ro; razvan.ungureanu@inflpr.ro; gabriel.cojocaru@inflpr.ro; mihai.serbanescu@inflpr.ro; aurelian.marcu@inflpr.ro; elena.stancu@inflpr.ro; alexandru.achim@inflpr.ro; marian.zamfirescu@inflpr.ro

Received

Abstract. CETAL-PW high power laser facility reports first accelerated electron beams with maximum energies up to ~500 MeV obtained in Romania, by focusing ultra-short laser pulses of 35 fs with energies up to 5 J before compression on supersonic gas jets of low-density He 99% - N2 1% mixture. The conditions for generation of stable electron beams (root mean square (rms) pointing stability of about 5 mrad), with different types of spectral characteristics and average maximum electron energies between 180 MeV and 380 MeV are presented. Maximum energies for all accelerated electron spectra are well described by theoretical estimations.

Key words: High-intensity ultra-short pulse laser, laser wake field acceleration, plasma wave

1. INTRODUCTION

Starting from ninety's when Tajima and Dawson have theoretically stated that it is possible to accelerate particles with high energy at the interaction of short ultra-intense laser pulses with under-dense plasma [1], a lot of progress has been achieved in this topic. Pukohov and Meyer-Ter-Vehn used three-dimensional particle-in-cell simulations to show that electron bunches with sharp peak energy around 300 MeV are possible to be generated from 12 J, 33 fs laser pulses [2]. If in early experimental studies, the electron beams produced from laser–plasma experiments have always been observed to have a large energy spread ($\Delta E/E$ ~100%) [3-5], nowadays the laser-plasma conditions are better controlled in order to obtain high quality, high energy electron beams [6-10]. However, stable, low energy spread and reliable monoenergetic electron beams still remain a desire for laser-plasma accelerators to be used in applications like, FEL, radiotherapy, etc. It was demonstrated experimentally and supported by simulations that the laser wake

field acceleration (LWFA) is enhanced when the self-injection of electrons is replaced by ionization injection which is initiated by doping the main gas (He or H) with impurities with higher atomic number, like nitrogen, argon, etc. Thus, the electrons are more efficiently trapped in the plasma accelerator which leads to enhanced beam stability, reduced energy spread and increased charge of the electron bunch [11-15]. A. Pak et al. present experimental evidence for the tunneling ionization injection and subsequent trapping of electrons into laser-produced wake-fields in a mixture of helium and trace amounts of nitrogen [12]. Song Li et al. observed an overall enhancement of a laser wake-field acceleration (LWFA) using the ionization injection in a mixture of 0.3% nitrogen gas in 99.7 % helium gas [13]. C. Thaury et al. used a shock front transition to localize the ionization injection in a gas mixture composed of 99% helium and 1% nitrogen [14].

CETAL-PW, (Romania) is hosting a Ti:Sa PW class laser (800 nm, 25 fs, 25 J, 0.1Hz) where recent experiments had as main result accelerated electron beams with maximum energies up to ~ 500 MeV, by focusing the laser pulse with an f/27 off-axis parabolic mirror (OAP) on supersonic gas jets.

In order to obtain a reliable and stable electron acceleration process, low-density He 99% - N2 1% mixture was used in all experiments. For some particular conditions, quasi-monoenergetic electron beams were obtained. In this paper we present the laser-plasma conditions (parameters), which led to obtaining electron beams with different types of spectral characteristics, highlighting the conditions for relatively stable quasi-monoenergetic electron beams. We show, also, that the maximum energies for all spectra are well predicted by scaling laws based on the main limiting processes of the acceleration: diffraction, depletion, and dephasing, as it was shown by Schlenvoight et al. [16].

2. LASER ACCELERATOR SETUP

The sketch of the experimental set-up is given in Fig. 1. For laser beam focusing (beam diameter of about 12 cm), an off-axis parabolic mirror (OAP) with a focal distance of 3.2 m and an incidence angle of 10º is used. In order to prevent ablation and safely dump the laser beam, the electron detection and characterization system was installed at a long distance from the gas jet, approx. 1.8 m, in an extension of the interaction chamber (IC) as it can be seen in Fig. 1.

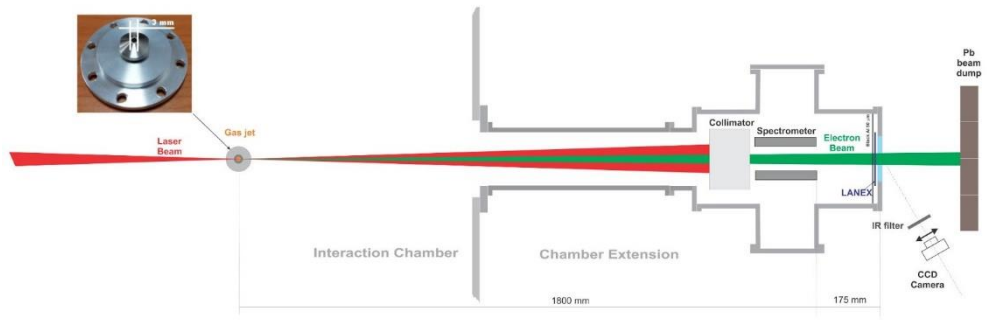

Fig. 1 – Experimental setup for CETAL-PW laser-gas jet interaction**.**

2.1. LASER BEAM CHARACTERIZATION SYSTEM AT THE TARGET LEVEL

At CETAL-PW lab, the laser beam is guided to the interaction chamber through a long (30 m) beam transport line with 4 dielectric mirrors. The propagation over such long distances and the complexity of the alignment process led to the need to implement an additional deformable mirror inside the IC together with a wavefront sensor (PHASICS), in order to maintain the quality of the laser beam. In order to improve the focal spot at the target level, both final optical compressor alignment manoeuvres (to correct chromatic aberrations) and wavefront corrections have been made. Fig. 2 (a) and (b) present an image and the spatial profile of the best focal spot obtained, with 35 **μ**m diameter and 35 % energy in the focal spot.

The stretcher of the chirped pulse amplification (CPA) system was adjusted for the best pulse compression and the pulse duration was measured at the IC level with a Wizzler ultrafast pulse measurement system [17]. Fig. 2 (c) presents the measured temporal profile of a 35 fs laser pulse.

2.2. TARGET: GAS JET

The gaseous target consists of supersonic (Mach 5) gas jets delivered in millisecond pulses by a gas valve and a 10° 3 mm Laval gas nozzle. The backing pressure was varied in the range 3 - 7 bar.

Gas density profiles measured by the wavefront sensor technique are presented in Fig. 3 for various delays with respect to the trigger signal applied to the controller unit of the gas valve. These results show that the gas starts to flow

after 4 ms from the trigger, reaching its maximum density between 5 and 6 ms. The effective gas pulse duration can be considered larger than 4 ms, as the density keeps over $1x10^{19}$ cm^{-3} up to 9 ms.

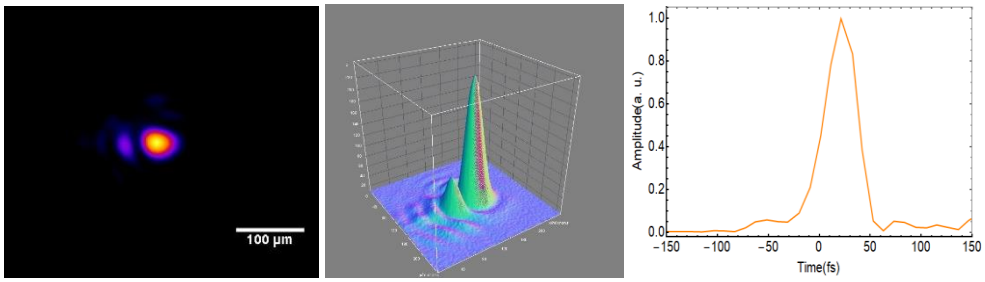

(a) (b) (c)

Fig. 2 – Image (a) and the spatial profile (b) of the best focal spot obtained, with 35 µm diameter and corrected chromatic aberrations; (c) temporal profile of the ultrashort laser pulse after best compression optimization, measured with the Fastlite Wizzler at the IC level [17].

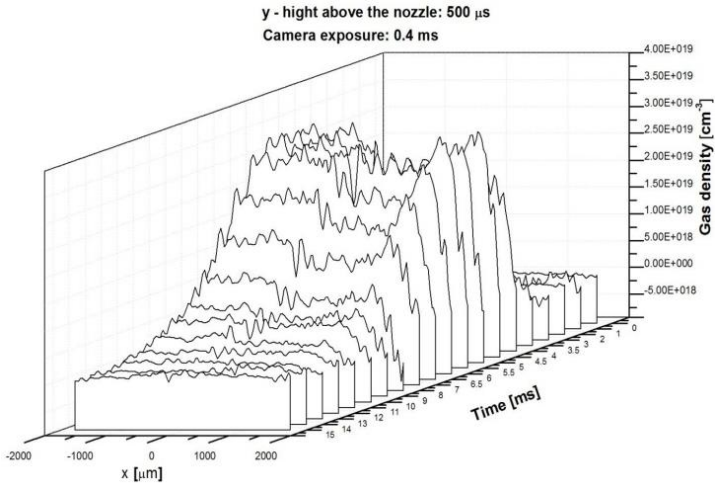

Fig. 3 – Time evolution of the spatial profile of the gas density.

2.3. ELECTRON BEAM CHARACTERIZATION SYSTEM

The accelerated electrons are detected with a scintillator screen (LANEX fast back) placed at the end of the IC extension (see Fig. 1), right on the extraction window. The light emitted from the LANEX screen is monitored with an optical

system with an f/2 objective having the focal distance 50 mm, placed on a CCD Basler camera.

The electron energy distribution is measured with a magnetic dipole electron spectrometer placed in the chamber extension, 175 mm before the circular LANEX screen with a 90 mm diameter, as it is shown in Fig. 4. A high-intensity magnetic field of 0.86 T is created by a dipole permanent magnet with a length of 80 mm and a gap of 10 mm. In order to define the entrance point in the magnetic field for those electrons that will be measured, a lead brick with 2 mm central pierce was used as a collimator and it was placed right before the magnetic spectrometer. Thereby, only those electrons entering this 2 mm orifice (~1.3 mrad at ~1.5 m from the gas jet to the lead brick) are selected and will be deviated on the scintillating screen. A sketch of the entire spectrometer setup is presented in Fig. 4. Taking into account all the parameters, a calibration curve was calculated based on the relativistic motion of electrons under the action of Lorentz force. The constructive design (only 90 mm diameter of the LANEX observation window) limits the minimum energy that can be measured at about 100 MeV, with a relative resolution ranging from dE/E ~ 5% (at 100 MeV) to > 20% (for E > 400 MeV).

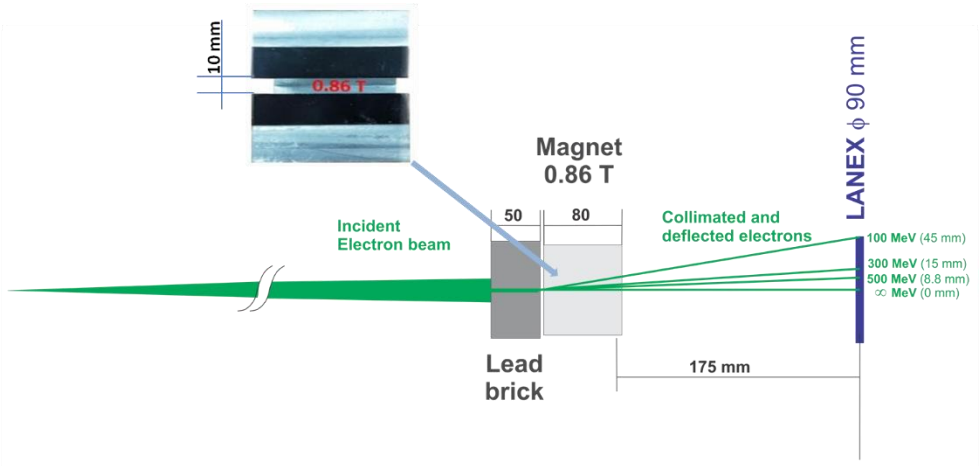

Fig. 4 – Sketch of the permanent magnets electron spectrometer with high magnetic field, B = 0.86 T.

3. ELECTRON BEAM MEASUREMENTS AND DISCUSSION

Accelerated electron beams were obtained for the first time in Romania, at CETAL-PW laboratory, INFLPR, in ultrashort (τ = 35 fs) laser pulse interaction

with He 99 % - N2 1% mixture gas jets. Laser pulses with energies up to 5 J before compression were focused with the f/27 OAP obtaining up to 1.2 J laser energy on the focal spot.

The electron beams were obtained for backing pressure in the range 4 - 6.5 bar, corresponding to a gas density, at 1.5 mm above the nozzle, in the range 3.2 - 5.2 x 10^{18} cm^{-3}. An example of an electron spot, obtained on the LANEX screen at laser-gas parameters mentioned above, is given in Fig. 5.

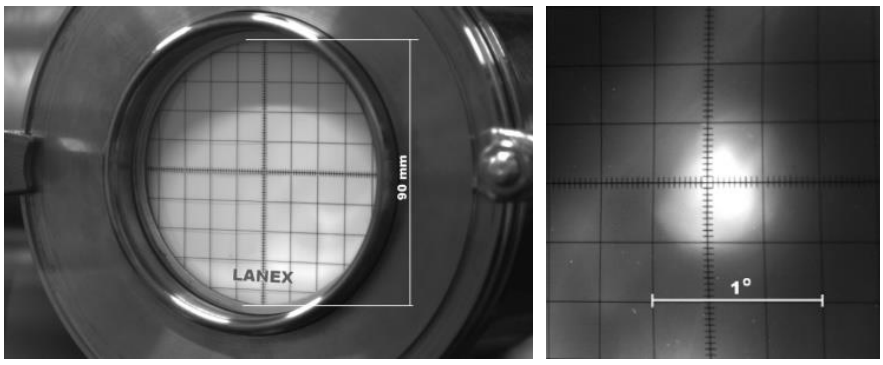

Fig. 5 – Scintillator screen placed on the extraction window of the IC extension - left; electron spot on LANEX screen of about 0.4º (~7 mrad) - right.

3.1. BEAM DIVERGENCE AND THE POINTING STABILITY

The best spot divergence was about 0.4º (~ 7 mrad), as can be seen in Fig. 5. Due to the laser beam pointing stability and random plasma filament formation, the electron beams jumped around in an angle of about 15 mrad (5 mrad root mean square (rms)). This can be seen in Fig. 6, where electron spot centroids distribution on LANEX is presented. These angular values are somewhere in the middle of the typical domains for the case of acceleration in gas jets and are in accordance with the characteristics obtained by other authors. For example, Maksimchuck et al. [8] obtained quasi-monoenergetic electrons with a beam divergence of 10 mrad and rms pointing stability of 7 mrad; Schlenvoigt et al. [16] mentioned about a mean deviation from the on-axis direction of about 40 mrad electron beam shot; Andre et al. [18] measured shot-to-shot pointing stability and obtained the shots distribution on the horizontal axis in an angle of about 11 mrad.

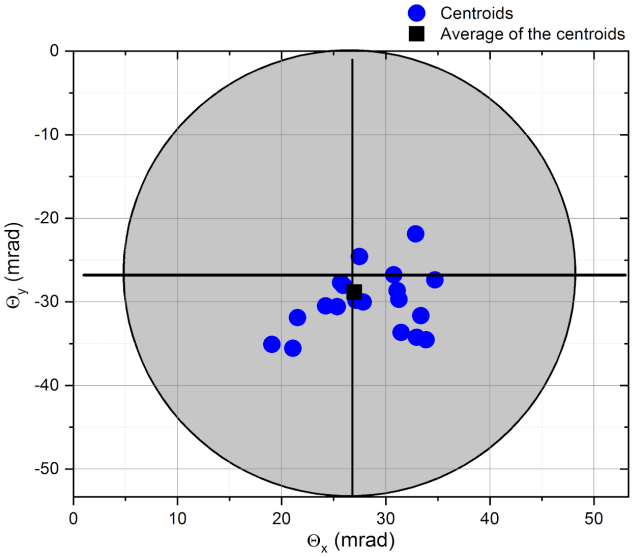

Fig. 6 – Electron spot centroids distribution on LANEX.

3.2. BEAM ENERGY DISTRIBUTION

Examples of electron spectra, measured with the high resolution spectrometer are presented in Fig. 7. Raw images (pictures) of the scintillating screen are presented in figures (a) - (d). Figure (e) shows the corresponding relative spectra. Absolute, calibrated, spectra will be given in a future work where a Faraday cup will be used to determine the charge of the electron beam [19]. Shots (a) - (d) corresponds to the following experimental conditions: (a) E_{LonF} = 1.26 J, e = 3.2 x 10^{18} cm^{-3}; (b) E_{LonF} = 1.16 J, n_e = 3.2 x 10^{18} cm^{-3}; (c) E_{LonF} = 1.06 J, n_e = 4.4 x 10^{18} cm^{-3}; (d) E_{LonF} = 1.06 J, n_e = 5.2 x 10^{18} cm^{-3}.

As it can be seen, different electron spectra shapes have been obtained, like multi-peak (a), continuous and a peak (E_{peak} = 370 MeV (b)), and single peak (quasi-monoenergetic) (c - d). The spectra shape is dependent on plasma density, ne, and laser pulse energy on focus, E_{LonF}. The strong dependence of the electron spectra shape on plasma density is observed by other authors, too. (e.g. Maksimchuk et al 2008 observed different spectra shapes with maximum energies up to 200 MeV when plasma density was varied in the range 7.5 x 10^{18} - 2.3 x 10^{19} cm^{-3}).

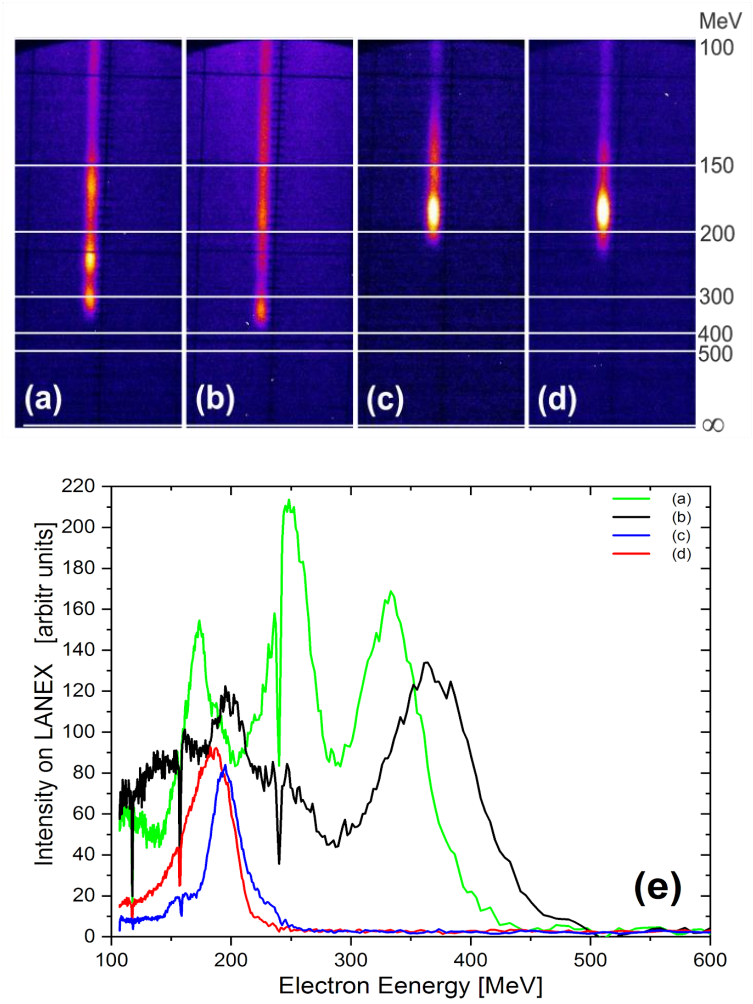

Fig. 7 – Electron spectra as raw data from the LANEX screen (a) $n_e = 3.2 \times 10^{18}$ cm^{-3} (b) $n_e = 3.2 \times 10^{18}$ cm^{-3}, (c) $n_e = 4.4 \times 10^{18}$ cm^{-3}, d) $n_e = 5.2 \times 10^{18}$ cm^{-3} and as corresponding relative spectra (e).

At CETAL-PW, electrons with quasi-monoenergetic distributions (single peak) are produced at laser pulse energy on target in focus E_{LonF} = 1.06 J for two different plasma densities. For plasma density $n_e = 4.4 \times 10^{18}$ cm^{-3} the electron peak energy is E_{peak} = 195 MeV with a full width at half-maximum σ(FWHM) = ± 14 MeV and for $n_e = 5.2 \times 10^{18}$ cm^{-3} the electron peak energy is E_{peak} = 183 MeV with σ(FWHM) = ± 23 MeV. In Fig. 8 these results are presented in comparison with other experimental data available in literature [6-10, 20].

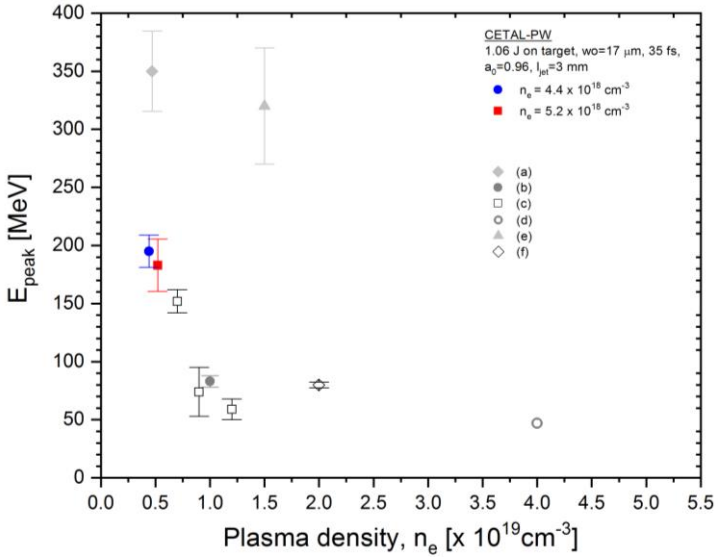

Fig. 8 – Peak electron energies obtained at CETAL-PW (red and blue symbols) and at other labs worldwide (black and gray symbols): (a) ALLS Canada, 2.4 J on target, 30 fs, w_0=11 mm, a_0=1.7, l_{jet}=5 mm [10]; (b) ALPHA X Univ. Strathclyde, 0.9 J on target, 35 fs, w_0=40 mm, a_0=1, l_{jet}=2 mm [9]; (c) 0.56 J after compressor, 54 fs, w_0= 8.4 x 9.2mm, a_0=1.3-1.4, l_{jet}=5 mm [20]; (d) JETI, 0.6J, 80 fs, w_0=1.6 mm, a_0= 5, l_{jet}= 0.65 mm [7]; (e) HERCULES, 1.2 J, 30 fs, w_0=9 mm, a_0= 2.2, l_{jet}= 2 mm [8]; (f) RAL, 0.5 J, 40 fs, w_0=12.5 mm, l_{jet}=2 mm [6].

In order to evaluate the stability of the electron source that is worth for applications, we did multi-shot measurements for the two density values (4.4 and 5.2 x 10^{18} cm^{-3}) and also for a few positions of the gas jet with respect to the laser focus position on z axis. The position of the optimum focal spot is denoted with z_0 and z_0+2mm and z_0+3mm correspond to positions closer to OAP. The results are gathered in a graph presented in Fig. 9. It can be observed that the peak electron energy fluctuates significantly. The energy stability is dependent on laser pulse energy which fluctuates up to +/- 12%, on plasma density fluctuation and plasma channel instability and also on the angular fluctuation of the electron beam while the entrance aperture (orifice of 2 mm) of the spectrometer was kept fixed. The last mentioned source of error is possible to be corrected in future works by a better design of the electron spectrometer.

For a better view, the average values of peak electron energy for different plasma densities and z positions (of the gas valve) are presented also as in Table 1.

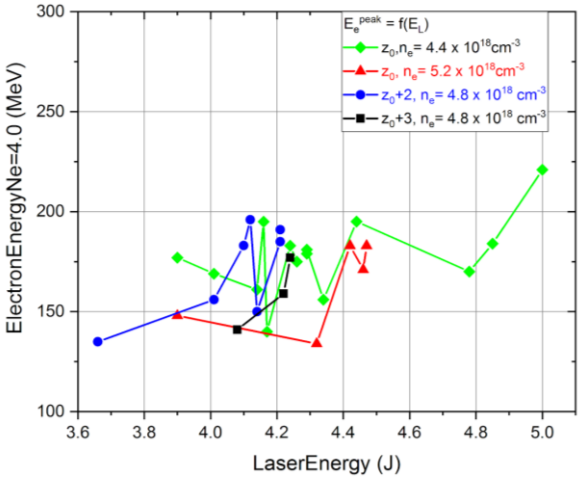

Fig. 9 – Peak electron energy as a function of laser energy; z_0 corresponds to focus position, whereas the higher values correspond to position closer to OAP.

Table 1

Average values of the peak electron energy for different plasma densities and z positions

Plasma density [x 10^{18} cm^{-3}]	*z position*	*Average of peak electron energy* [MeV]
4.4	z_0	**177.6 +/- 40**
5.2	z_0	**163.8 +/- 24**
4.8	z_0 + 2 mm (towards OAP)	**170.9 +/- 30**
4.8	z_0 + 3 mm (towards OAP)	**159.0 +/- 18**

3.2. MAXIMUM ENERGY GAIN

For maximum electron energy estimation (E_{max}), all Lanex screen images, captured at every set of laser shots, were processed with the ImageJ software in order to measure the electron deviations from the central beam axis. The maximum electron energy corresponds to the lowest deviation on the Lanex screen. For each set of experimental data, an average value of maximum electron energy $<E_{max}>$ was obtained and the corresponding deviations from the mean, δE_{max}. In Fig. 13,

the experimental average values of the maximum electron energies (full symbols) are presented as a function of the plasma density.

By applying the scaling laws (e.g. Ref. [16], the maximum energy gain E_{max} can be easily estimated for different sets of laser-plasma parameters, as in the following relation:

$$E_{max} \sim \sqrt{2}\frac{n_c}{n_e}\begin{cases}\pi a_0, & {a_0}^2 \ll 1\\ \dfrac{{a_0}^2}{3}, & {a_0}^2 \gg 1\end{cases} \quad (1)$$

where n_c is the critical density (density at which the laser cannot propagate anymore through plasma).

For comparison with experimental data, $<E_{max}>$ values were calculated for the same laser-plasma conditions used in the experimental campaign, i.e. laser energies from the experimental campaign, BTL transmission of 60 %, a fraction of energy on focus (SR) = 35 %, n_e from 3.2 to 5.2 x10^{18} cm^{-3}, laser pulse duration 35 fs, laser spot diameter 35 μm. The results are given with open symbols in Fig. 10. As can be seen, the experimental data are well described by theoretical estimations. The differences between calculation and experiment are in the range of error bars, the theory giving a little bit higher electron energy gains at the same plasma densities and laser conditions used in the experimental campaign.

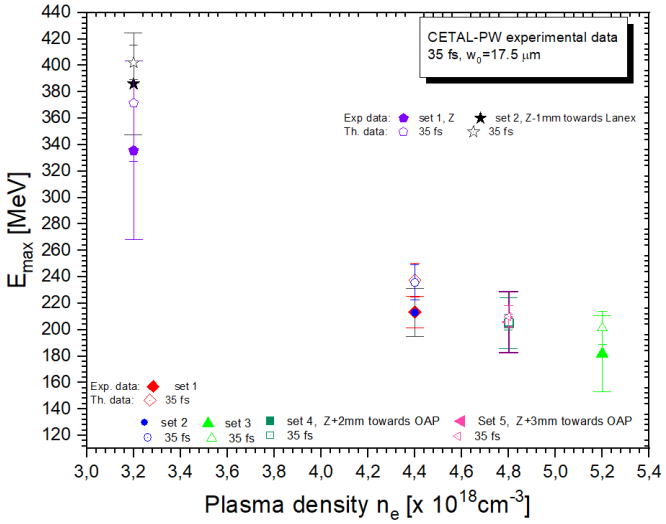

Fig. 20 – Average maximum electron energies: experimental data (full symbols) and present calculation (open symbols).

4. CONCLUSIONS

Laser-plasma accelerated electrons were obtained for the first time in Romania at CETAL-PW high-power laser facility of National Institute for Lasers, Plasma and Radiation Physics (INFLPR).

Electrons with energy distributions of different shapes and with maximum energies up to ~ 500 MeV have been accelerated by high-intensity laser interaction with supersonic gas jet of low-density He 99% - N_2 1% mixture. The best beam divergence was about 7 mrad and rms pointing stability of about 5 mrad. Three types of electron spectra were measured: multi-peak, quasi-monoenergetic and spectrum with both continuous and peaky parts. Quasi-monoenergetic electron beams with peak energy up to 195 ± 14 MeV were obtained at laser pulse energy in the focus of E_{LonF} = 1.06 J and plasma density $n_e = 4.4 \times 10^{18}$ cm^{-3}.

The maximum electron energies have been measured up to 500 MeV at single-shot analysis. For a set of 10-30 shots, average maximum electron energy with values ranging between 180 MeV and 380 MeV were obtained. These results are well described by theoretical estimation.

In a future work, we aim to improve both, the control of laser parameters and the design of the electron spectrometer to characterize the electron beams with a higher degree of accuracy, according to the requirements of the main applications of these electron beams.

Aknowledgements. This work was supported by Romanian Ministry of Education and Research, under Romanian National Nucleu Program LAPLAS VI - contract no. 16N/2019, ELI- RO 5.1 program in the frame of PNCDI III 2015-2020 - contract no. 24/2016 and contract no. 27/2017 and PN-III-P4-ID-PCCF-2016-0164 nr. 8/2018.

REFERENCES

1. Tajima, J. Dawson, *Phys. Rev. Lett.* **43**, 267 (1979)
2. A. Pukhov, J. Meyer-Ter-Vehn, *Appl. Phys. B* **74**, 355 (2002)
3. D. Umstadter, *Phys. Plasma*, **8**, 1774 (2001)
4. V. Malka, S. Fritzler, E. Lefebvre, M-M. Aleonard, F. Burgy, J-P. Chambaret, J-F. Chemin, K. Krushelnick, G. Malka, S. P. D. Mangles, Z. Najmudin, M. Pittman, J-P. Rousseau, J-N. Scheurer, B. Walton, A. E. Dangor, *Science* **298**, 1596 (2002)
5. S. P. D. Mangles, B. R. Walton, M. Tzoufras, Z. Najmudin, R. J. Clarke, A. E. Dangor, R. G. Evans, S. Fritzler, A. Gopal, C. Hernandez-Gomez, W. B. Mori, W. Rozmus, M. Tatarakis, A. G. R. Thomas, F. S. Tsung, M. S. Wei and K. Krushelnick, *Phys. Rev. Lett.* **94**, 245001 (2005)

6. S. P. D. Mangles, C. D. Murphy, Z. Najmudin, A. G. R. Thomas, J. L. Collier, A. E. Dangor, E. J. Divall, P. S. Foster, J. G. Gallacher, C. J. Hooker, D. A. Jaroszynski, A. J. Langley, W. B. Mori, P. A. Norreys, F. S. Tsung, R. Viskup, B. R. Walton and K. Krushelnick, *Nature* **431**, 535 (2004)
7. B. Hidding, K-U. Amthor, B. Liesfeld, H. Schwoerer, S. Karsch, M. Geissler, L. Veisz, K. Schmid, J. G. Gallacher, S. P. Jamison, D. Jaroszynski, G. Pretzler and R. Sauerbrey, *Phys. Rev. Lett*. **96**, 105004 (2006)
8. A. Maksimchuk, S. Reed, S. S. Bulanov, V. Chvykov, G. Kalintchenko, T. Matsuoka, C. McGuffey, G. Mourou, N. Naumova, J. Nees, P. Rousseau, V. Yanovsky, K. Krushelnick, N. H. Matlis, S. Kalmykov, G. Shvets, M. C. Downer, C. R. Vane, J. R. Beene, D. Stracener, D. R. Schultz, *Phys. Plasmas* **15**, 056703 (2008)
9. S. M. Wiggins, R. P. Shanks, R. C. Issac, G. H. Welsh, M. P. Anania, E. Brunetti, G. Vieux, S. Cipiccia, B. Ersfeld, M. R. Islam, R. T. L. Burgess, G. Manahan, C. Aniculaesei, W. A. Gillespie, A. M. MacLeod, D. A. Jaroszynski, *Plasma Phys. Control. Fusion* **52**, (12) (2010)
10. P. A. Masson-Laborde, M. Z. Mo, A. Ali, S. Fourmaux, P. Lassonde, J. C. Kieffer, W. Rozmus, D. Teychenné, R. Fedosejevs, *Physics of Plasmas* **21**, 123113-1 (2014)
11. C. McGuffey, A. G. R. Thomas, W. Schumaker, T. Matsuoka, V. Chvykov, F. J. Dollar, G. Kalintchenko, V. Yanovsky, A. Maksimchuk, K. Krushelnick, Yu. V. Bychenkov, I. V. Glazyrin, A. V. Karpeev, *Phys. Rev. Lett.* **104**, 025004 (2010)
12. A. Pak, K. A. Marsh, S. F. Martins, W. Lu, W. B. Mori, C. Joshi, *Phys. Rev. Lett.* **104**, 025003 (2010)
13. S. Li, N. A. M. Hafz, M. Mirzaie, T. Sokollik, M. Zeng, M. Chen, Z. Sheng and J. Zhang, *Cornell University, arXiv*: 1410.2331 (2014)
14. C. Thaury, E. Guillaume, A. Lifschitz, K. Ta Phuoc, M. Hansson, G. Grittani, J. Gautier, J-P. Goddet, A. Tafzi, O. Lundh and V. Malka, *Scientific Reports* **5**, 16310 (2015)
15. Y-C. Ho, T-S. Hung, C-P. Yen, S-Y. Chen, H-H. Chu, J-Y. Lin, J. Wang, M-C. Chou, *Phys. Plasmas* **18**, 063102 (2011)
16. H-P. Schlenvoigt, O. Jackel, S. M. Pfotenhauer and M. C. Kaluza, "*Laser-based Particle Acceleration*", M. Grishin ed, "*Advances in Solid-State Lasers: Development and Applications"*, INTECH, Croatia, 630, 2010.
17. T. Oksenhendler, P. Bizouard, O. Albert, S. Bock, U. Schramm, *Opt. Express* **25**, 12588-12600 (2017)
18. T. Andre, A. Andriyash, A. Loulergue, M. Labat, E. Roussel, A. Ghath, M. Khojoyan, C. Thaury, M. Valléau, F. Briquez, F. Marteau, K. Tavakoli, P. N'Gotta, Y. Dietrich, G. Lambert , V. Malka, C. Benabderrahmane, J. Vétéran, L. Chapuis, T. El Ajjouri, M. Sebdaoui, N. Hubert, O. Marcouillé, P. Berteaud, N. Leclercq, M. El Ajjouri, P. Rommeluère, F. Bouvet, J-P. Duval, C. Kitegi, F. Blache, B. Mahieu, S. COrde, J. Gautier, K. Ta. Phuoc, J. P. Goddet, A. Lestrade, C. Herbeaux, C. Évain, C. Szwaj, S. Bielawski, A. Tafzi, P. Rousseau, S. Smartsev, F. Polack, D. Dennetière, C. Bourassin-Bouchet, C. De Oliveira and M-E. Couprie, *Nature Communications* **9**, 1334 (2018)
19. D. Ticos, A. Scurtu, M. Oane, C. Diplasu, G. Giubega, I. Calina, C. M. Ticos, *Results in Physics* **14**, 102377 (2019)
20. J. Kim, Y. H. Hwangbo and S-Y. Lee, *Journal of the Korean Physical Society* **71**, 256 (2017)